

Cryptic insertions of the immunoglobulin light chain enhancer region near *CCND1* in t(11;14)-negative mantle cell lymphoma

Cyclin D1+ mantle cell lymphoma (MCL) is molecularly characterized by the t(11;14)(q13;q32) or rearrangements of *CCND1* gene with the immunoglobulin (IG) light chains.^{1,2} Most MCL can be diagnosed based on the characteristic pathologic features and cyclin D1 expression without the need for demonstrating the genetic translocation. However, in cases with atypical morphologic or phenotypic features other B-cell neoplasms that sometimes also have cyclin D1 positivity may be in the differential diagnosis.¹ In these situations the detection of the *CCND1* rearrangements may assist in the diagnosis since most other lym-

phomas do not carry translocations of the gene.³⁻⁷ A subset of plasma cell myelomas express cyclin D1 associated with the t(11;14) but are usually not in the differential diagnosis of MCL and are SOX11-negative.⁵ Nevertheless, there are occasional lymphoid neoplasms with MCL features in which cyclin D1 is strongly expressed without an apparent gene rearrangement detected using conventional cytogenetics or fluorescence *in situ* hybridization (FISH) with fusion or break-apart probes. The mechanisms of cyclin D1 overexpression in these cases are unclear and the MCL diagnosis may be questioned.

In this study, we have identified four MCL and one mature B-cell lymphoma with marked plasmacytic differentiation with strong cyclin D1 overexpression but in which *CCND1* rearrangements could not be detected by

Table 1. Clinical and pathological data of the five Cyclin D1+ B-cell lymphomas.

	Case 1 (index)	Case 2	Case 3	Case 4	Case 5
Age/gender	72/M	67/M	70/M	60/M	71/M
Lymphocytosis	No	NA	No	Yes	Yes
LDH increased	No	NA	Yes	No	NA
LN involvement	Yes	Yes	Yes	No	Yes
PB involvement	Yes	No	Yes	Yes	Yes
BM involvement	Yes	Yes	Yes	Yes	Yes
Splenomegaly	NA	No	Yes	Yes	Yes
GI involvement	Yes	Yes	Yes	No	No
Stage	IV A	IV A	IV B	IV A	IV A
First line treatment	R-Benda+ Ibrutinib	Immunoche motherapy	R-CHOP	Abstention/ R-Ibrutinib	Multiple Chemotherapy ^a
Response	Complete	Unknown	Refractory	Under treatment	Partial
Relapse (months)	Colon (36 m)	No	No	No	Lymphadenopathy High IgM paraprotein ^b (120 m)
Follow up (months)	AWD (62 m)	DD (108 m)	AWD (7 m)	Alive, (42 m)	DD (130 m)
Biopsy site	Colon	LN	LN	BM	LN
Growth pattern	NA	Nodular/ Diffuse	Diffuse	Interstitial	Diffuse
Morphology	Classic	Classic	Pleomorphic/Classic	Small cell	Small cell with plasmacytic differentiation
CD20	+	+	+	+	+
CD5	+	+	+	- BM/+ PB	-
CD23	-	-	-	-	-
Cyclin D1	+	+	+	+	+
SOX11	+	+	-	-	-
Light chain restriction	Kappa	Lambda	Kappa	Kappa	Kappa
IgD	ND	ND	-	+	-
Ki67 (%)	30	30-40	>50	10-30	Very variable
FISH <i>CCND1</i> BAP	- (BM)	-	-	-	-
FISH <i>CCND1</i>					
Fusion	- (Colon)	-	-	-	-
FISH IGKenh/ <i>CCND1</i>	+ (BM)	+	+	-	-
FISH <i>CCND1</i> /IGLenh	ND	ND	ND	+	-

AWD: alive with disease; FISH: fluorescence *in situ* hybridization; BAP: break-apart FISH probe; BM: bone marrow; DD: dead of disease; LN: lymph node; M: male; NA: not applicable; ND: not done; PB: peripheral blood; GI: gastrointestinal involvement; +: positive; -: negative. ^aChlorambucil (2010), splenectomy and R-CVP (2011), R-CHOP (2012), Ofatumumab (2013), Velcade, cyclophosphamide and dexamethasone (2014). ^bIncreasing IgM paraprotein throughout the course of disease (3.7 g/L in 2005, 11.2 g/L in 2011 and 80 g/L in the final phases).

conventional cytogenetics or FISH using fusion or break-apart probes. To determine the mechanism leading to cyclin D1 overexpression in these cases we analyzed the index case by whole-genome sequencing (WGS) followed by FISH studies with custom probes for the IG light chain enhancer regions in all cases and demonstrated the presence of cryptic translocations of the enhancer region of the IG light chains with *CCND1* in the four cyclin D1-positive MCL.

The study was approved by the Institutional Review Board of the Hospital Clinic of Barcelona and informed consent was obtained in accordance with the Declaration of Helsinki. Lymphomas were studied by immunohistochemistry with a panel of antibodies (*Online Supplementary Materials and Methods and Online Supplementary Table S1*) and reviewed by four pathologists. Tumor genomic DNA was isolated from formalin-fixed paraffin-embedded tissue biopsies (cases 2, 3, and 5), fresh bone marrow aspirate (case 1) and peripheral blood cells (case 4). Paired-end WGS was performed on tumor and germline DNA from case 1 (index case) using standard Illumina protocols and analyzed as previously described.⁸ *CCND1* rearrangement was analyzed by FISH using *CCND1* and IG commercial and custom BAC-labeled probes (*Online Supplementary Table S2*). Copy number alterations were investigated using Oncoscan FFPE or SNP6.0 (ThermoFisher Scientific, Waltham, MA, USA).^{9,9} The mutational status of 115 genes was examined by targeted next-generation sequencing (NGS) (*Online Supplementary Table S3*).¹⁰ Further details can be found in *Online Supplementary Materials and Methods*.

The clinical and pathological features of the patients are summarized in Table 1. All patients were in stage IV with peripheral blood and bone marrow involvement. Cases 1-3 presented with generalized lymphadenopathy, whereas case 4 had asymptomatic lymphocytosis and splenomegaly. Case 5 had an unusual clinical history and evolution. The patient was exposed to extensive radiation

due to atomic bomb tests in the early 1960s and developed several solid tumors (thyroid papillary carcinoma, basal cell carcinoma, melanoma and pleomorphic sarcomas) that were treated without further relapses. In 2003 he was diagnosed with a lymphoproliferative disorder consistent with atypical chronic lymphocytic leukemia which did not require treatment until 2010, when chlorambucil was started. Two years later the patient developed splenomegaly and lymphadenopathy, that was biopsied. The bone marrow biopsy from 2005 showed a nodular and interstitial lymphoid infiltration. The patient had an IgM lambda paraprotein, which was stable for several years but progressively increased in the final phases of the disease. The patient required several lines of therapy without response and died of progressive disease 11 years after the initial diagnosis. The other four patients received different treatments. Case 2 died of disease and cases 1, 3, and 4 were alive at the last follow-up.

Cases 1 and 2 had classic MCL cytology, whereas case 3 showed a large cell pleomorphic component with unusual clear cytoplasm intermingled with abundant atypical small cells. Cyclin D1 was strongly positive in both components. Case 4 had small cell morphology and case 5 showed small cells with marked plasmacytic differentiation and occasional Dutcher bodies (Figure 1). CD5 was positive in all cases except in case 5 and the bone marrow cells of case 4. SOX11 was positive in cases 1 and 2 and negative in cases 3 to 5. Four cases had kappa light chain restriction and case 2 expressed lambda. Case 5 had strong cytoplasmic IgM/kappa expression (Table 1).

All cases were negative for *CCND1* rearrangements by FISH using commercial fusion and break-apart probes on the diagnostic biopsies (Table 1 and *Online Supplementary Figure S1A-B*). In cases 1 and 5 the FISH analyses were performed in multiple samples. The karyotype in case 1 was 46,XY,der(11)t(3;11)(q13;q25)[9]/46,XY[11]. The unbalanced chromosome 11 translocation with chromosome 3

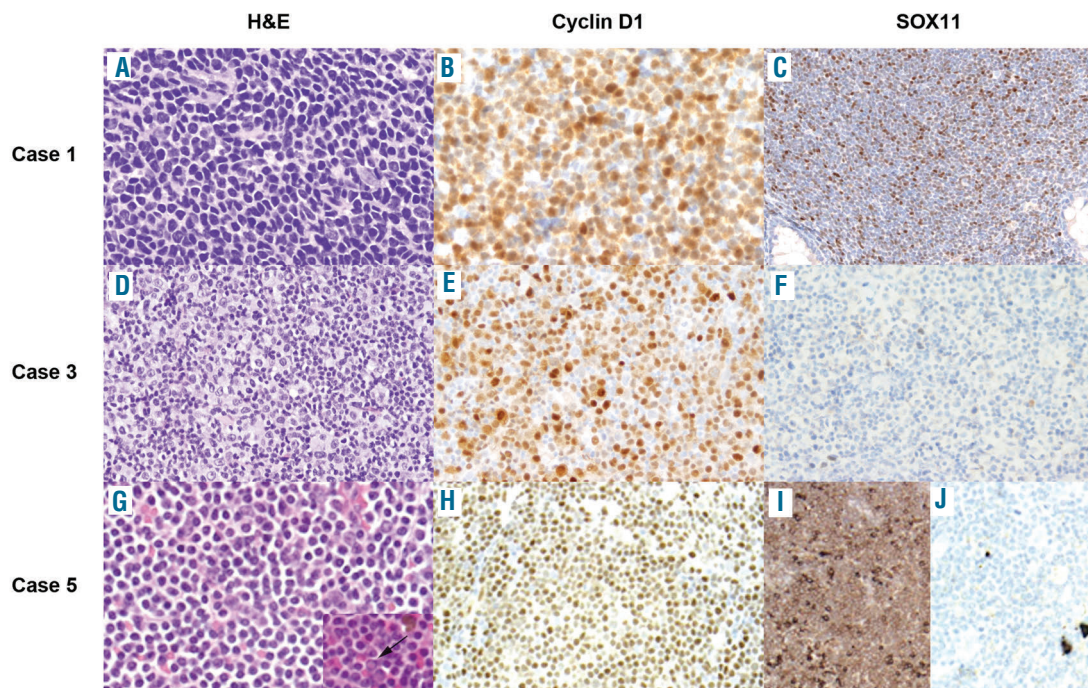


Figure 1. Morphological and phenotypic features of cases 1, 3, and 5. (A, B, C) Case 1, hematoxylin and eosin (40x) (A), positive cyclin D1 (40x) (B), positive SOX11 expression (10x) (C). (D, E, F) Case 3, hematoxylin and eosin (20x) (D), positive cyclin D1 (20x) (E), negative SOX11 expression in large and medium cells in case 3 (20x) (F). (G, H, I, J) Case 5, hematoxylin and eosin with occasional Dutcher bodies (inset) (20x) (G), positive cyclin D1 (10x) (H), kappa light chain restriction (10x) (I) and lambda negative (10x) (J).

did not involve the *CCND1* locus (11q13), and was further confirmed by whole chromosome painting (Online Supplementary Figure S2). Case 2 had a complex karyotype, 44-46,XY,-Y[2], del(6)(q21q23), del(7)(p15p22), add(9)(p11.2), del(11)(q21q23.1), del(13)(q11q34)[2], add(22)(p11.2)[6][cp7]/46,XY[9], without the t(11;14) translocation.

We performed WGS of case 1 and identified a rearrangement involving IGK in chromosome 2 and *CCND1* in chromosome 11. A 412 Kb region of the IGK, including the IGK enhancer (IGKenh) and the IGK constant (IGKC) region was inserted 226.3 Kb upstream of *CCND1* gene (Figure 2A-B). We confirmed the rearrangement by PCR, Sanger sequencing and FISH using custom fusion probes combining *CCND1* gene (red) and IGKenh probes (green) that we had used previously (Figure 2C).⁸ FISH using the commercial IGK break-apart probe confirmed the rearrangement detected by WGS (Online Supplementary Figure 1C). The finding of the cryptic rearrangement of IGK with *CCND1* in case 1, prompted us to analyze this cryptic rearrangement in the remaining four cases by FISH. The IGKenh/*CCND1* rearrangement was also detected in cases 2 and 3, both in the small and large cells (Figure 2D-E). However, cases 4 and 5 were negative. We next tested the combination of *CCND1* with IGLenh and case 4 was positive (Figure 2F) whereas case 5 was negative for both IGKenh and IGLenh with *CCND1* probes.

Targeted sequencing identified mutations in 24 different genes (Online Supplementary Table S4). Cases 1-3 had mutations already reported in MCL,⁹ including *ATM*, *TP53*, *NOTCH2*, *KMT2D*, *NFKBIE*, *ARID1A*, *SMARCA4*, and *CARD11*. Case 4 had mutations in *KLHL6*, *DTX1* and *SETD2*, whereas case 5 had a clonal (allelic frequency of 44.4%) p.L265P *MYD88* mutation (Online Supplementary Figure S3). The genomic profile was complex in cases 1 to 3 with copy number alterations commonly found in MCL (+3q, -9p, -9q, -11q, -13q, and -17p), whereas case 4 did not show any copy number alterations, in line with its indolent clinical course and SOX11-negativity (Online Supplementary Table S5). Case 5 showed eight copy number alterations including +2p, +17q, -6q and -9p.

In summary, cyclin D1 overexpression in 4 of 5 cases was associated with cryptic *CCND1* rearrangements that involved the enhancers of IGK and IGL in three cases and one case, respectively. Similar to conventional rearrangements with IGH, the IG light chain translocated fragments (including the enhancers) could be responsible for the dysregulation of cyclin D1 in MCL. These findings are similar to our recent observations in cyclin D1-negative MCL overexpressing cyclin D2 or cyclin D3 which carried cryptic insertions of the IGK and IGL enhancers near *CCND2* or *CCND3*, respectively.⁸ The detection of cryptic rearrangements of *MYC* and *BCL2* with regulatory regions of IG genes has been recently reported in B-cell neoplasms.¹¹⁻¹⁵

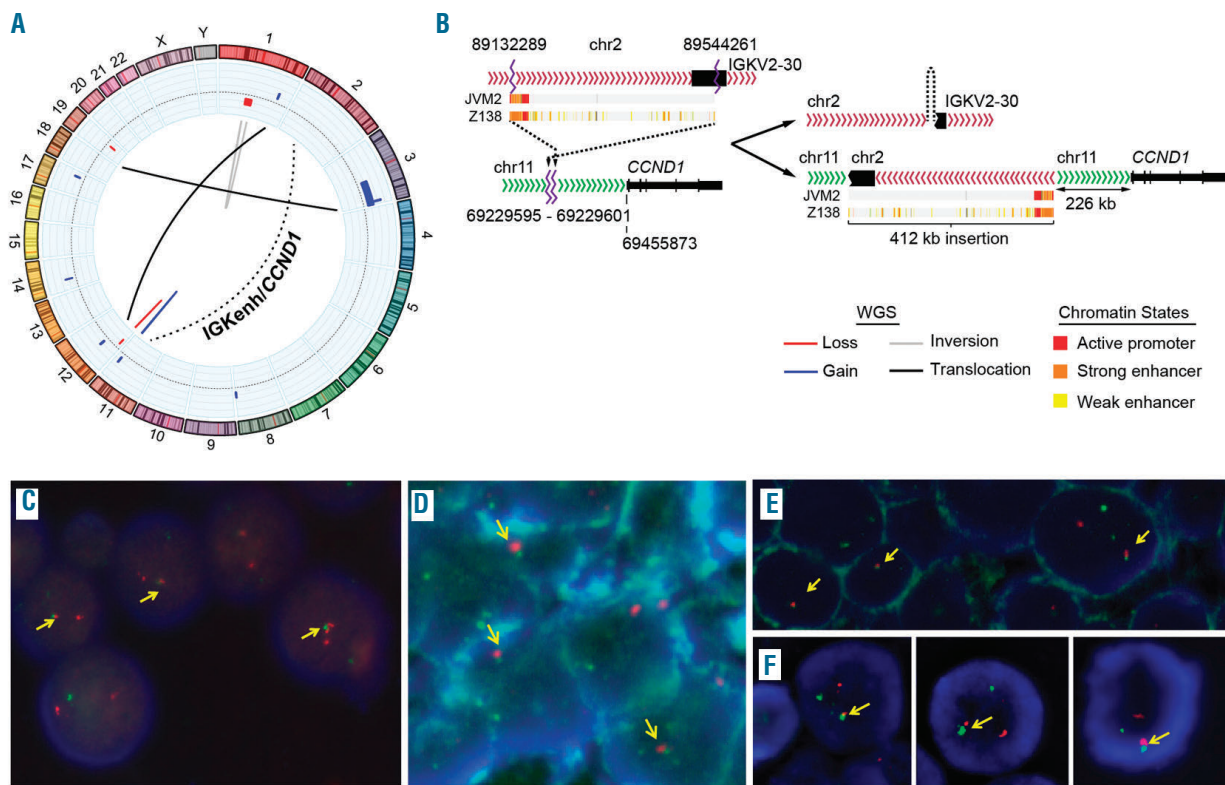


Figure 2. Cryptic insertions of IG light chain genes near *CCND1* gene. (A-C) case 1. (A) Circos plot with copy number alterations (blue for gains and red for losses) in the outer circle and structural variants detected by whole-genome sequencing. The interchromosomal (black lines) and intrachromosomal (blue for gain, red for loss, grey for inversion) rearrangements are represented in the inner circle. The rearrangement between chr2 (IGKenh) and chr11 (*CCND1*) is indicated with a dashed line. (B) Schematic representation of IGK (chr2) and *CCND1* (chr11) loci in normal cells (left) and derivative chromosomes after the rearrangement (right). The rearrangement consisted of an inverted insertion of IGK 226 Kb upstream of *CCND1* gene. The chromatin states in two MCL cell lines (Z138 and JVM2) were displayed for the entire fragment of IGK inserted region, the orange part represents the enhancer region which was placed proximal to *CCND1* coding region. (C) Verification of the cryptic IGKenh/*CCND1* insertion by FISH using the custom fusion probe IGKenh (green) and *CCND1* (red). Juxtaposition of one red and one small green signals was observed in most cells (yellow arrows). (D-F) Fluorescence *in situ* hybridization (FISH) verification of cryptic *CCND1* rearrangements in cases 2 to 4. Cells positive for the cryptic rearrangement IGKenh/*CCND1* in case 2 (D) and case 3 (E), including medium and large cells. (F) Cells positive for the cryptic rearrangement *CCND1*/IGLenh in case 4. In all cases the juxtaposition of one red and one green signal was highlighted with yellow arrows.

The findings in case 5 were intriguing and specific taxonomic classification of the tumor was difficult. The IgM, kappa paraprotein and plasmacytic differentiation was consistent with a lymphoplasmacytic lymphoma, and concordantly the tumor carried the p.L256P MYD88 mutation. However, cyclin D1 was diffusely expressed without evidences of CCND1 rearrangements. The lack of CCND1 rearrangement detection with our probes does not completely rule out other alternative rearrangements. In this sense, a recent study of a MCL without apparent CCND1 rearrangements has detected an insertion of the entire CCND1 coding region into the IGH locus which was not detected by standard probes and would not have been detected with our IG light chain probes.¹⁴ The characteristics of our case with marked plasmacytic differentiation, strong cyclin D1 expression and MYD88 mutation are similar to a previously reported case but in which the t(11;14) could be demonstrated by FISH.¹⁵ Whether these cases should be classified as lymphoplasmacytic lymphoma with CCND1 rearrangements or MCL with MYD88 mutations is debatable. Independent of the possible taxonomy of these tumors, it is important to recognize their clinical and biological peculiarities.

In conclusion, cryptic translocations of the IG light chain regulatory region with CCND1 may be an alternative mechanism to deregulate this gene in MCL. FISH testing for the IG light chain enhancer region could be incorporated into the diagnostic work up of MCL negative for the t(11;14) or CCND1 rearrangements with standard probes, especially in cases with atypical pathological or clinical features.

Carla Fuster,^{1*} David Martín-García,^{2,3*} Olga Balagué,^{1,4} Alba Navarro,^{2,3} Ferran Nadeu,^{2,3} Dolors Costa,^{1,3} Miriam Prieto,² Itziar Salaverria,^{2,3} Blanca Espinet,⁵ Alfredo Rivas-Delgado,^{2,6} Maria José Terol,⁷ Eva Giné,^{2,3,6} Pilar Forcada,⁸ Margaret Ashton-Key,⁹ Xose S. Puente,^{3,10} Steven H. Swerdlow,¹¹ Silvia Bea^{1,2,3,4#} and Elias Campo^{1,2,3,4#}

*CF and DMG contributed equally as co-first authors.

#SB, EC contributed equally as co-senior authors.

¹Hematopathology Section, Laboratory of Pathology, Hospital Clínic de Barcelona, Barcelona, Spain; ²Institut d'Investigacions Biomèdiques August Pi i Sunyer (IDIBAPS), Barcelona, Spain; ³Centro de Investigación Biomédica en Red de Cáncer (CIBERONC), Madrid, Spain; ⁴University of Barcelona, Barcelona, Spain; ⁵Laboratori de Citogenètica Molecular, Servei de Patologia, Hospital del Mar, Barcelona, Spain; ⁶Grup de Recerca Translacional en Neoplàsies Hematològiques, Cancer Research Programme, IMIM-Hospital del Mar, Barcelona, Spain; ⁷Department of Hematology Hospital Clínic de Barcelona, Barcelona, Spain; ⁸Department of Hematology, Hospital Clínic, INCLIVA Biomedical Research Institute, University of Valencia, Valencia, Spain; ⁹Department of Pathology, Hospital Mutua Terrassa, Terrassa, Spain; ¹⁰Department of Cellular Pathology, Southampton University Hospitals National Health Service Trust, UK; ¹¹Departamento de Bioquímica y Biología Molecular, IUOPA, Universidad de Oviedo, Oviedo, Spain and ¹²Department of Pathology, University of Pittsburgh School of Medicine, Pittsburgh, PA, USA

Acknowledgments: the authors would like to thank the IDIBAPS Genomics Core Facility and the Hematopathology Collection from the Hospital Clínic/IDIBAPS; the Molecular Cytogenetic Platform of IMIM, Hospital del Mar (Barcelona) for providing one IGH BAC clone. Miriam Prieto, Silvia Martín, Cándida Gómez, and Amparo Arias for their excellent technical assistance and Montserrat Puiggròs and Romina Royo from the Barcelona SuperComputing Center. This work was developed at the Centro Esther Koplowitz (CEK), Barcelona, Spain

Funding: this work was supported by research funding from Fondo de Investigaciones Sanitarias, Instituto de Salud Carlos III PI17/01064 (SB), Ministerio de Ciencia y Innovación RTI2018-094274-B-I00 (EC), SAF2017-87811-R (XSP) from Plan Nacional de I+D+I, the NIH grant number 1 P01CA229100 (EC), Generalitat de Catalunya Suport Grups de Recerca 2017-SGR-709 (SB), 2017-SGR-1142 (EC), and the European Regional Development Fund "Una manera de fer Europa", CERCA Programme/Generalitat de Catalunya. EC is an Academia Researcher of the "Institució Catalana de Recerca i Estudis Avançats" of the Generalitat de Catalunya. Miriam Prieto is supported by "Acció instrumental d'incorporació de científics i tecnòlegs PERIS 2016" (SLT002/16/00347) from Generalitat de Catalunya. Alfredo Rivas-Delgado is supported by "Josep Font" grant from Hospital Clínic de Barcelona

Correspondence: SILVIA BEA/ELIAS CAMPO
sbea@clinic.cat/ecampo@clinic.cat

doi:10.3324/haematol.2019.237073

Information on authorship, contributions, and financial & other disclosures was provided by the authors and is available with the online version of this article at www.haematologica.org.

References

- Sander B, Quintanilla-Martinez L, Ott G, et al. Mantle cell lymphoma: a spectrum from indolent to aggressive disease. *Virchows Arch.* 2016;468(3):245-257.
- Wlodarska I, Meeus P, Stul M, et al. Variant t(2;11)(p11;q13) associated with the IgK-CCND1 rearrangement is a recurrent translocation in leukemic small-cell B-non-Hodgkin lymphoma. *Leukemia.* 2004;18(10):1705-1710.
- Bosch F, Campo E, Jares P, et al. Increased expression of the PRAD-1/CCND1 gene in hairy cell leukaemia. *Br J Haematol.* 1995; 91(4):1025-1030.
- Chen BJ, Ruminy P, Roth CG, et al. Cyclin D1-positive Mediastinal Large B-Cell Lymphoma With Copy Number Gains of CCND1 Gene: A Study of 3 Cases With Nonmediastinal Disease. *Am J Surg Pathol.* 2019;43(1):110-120.
- Chen YH, Gao J, Fan G, Peterson LC. Nuclear expression of sox11 is highly associated with mantle cell lymphoma but is independent of t(11;14)(q13;q32) in non-mantle cell B-cell neoplasms. *Mod Pathol.* 2010;23(1):105-112.
- Hsiao SC, Cortada IR, Colomo L, et al. SOX11 is useful in differentiating cyclin D1-positive diffuse large B-cell lymphoma from mantle cell lymphoma. *Histopathology.* 2012;61(4):685-693.
- Vela-Chavez T, Adam P, Kremer M, et al. Cyclin D1 positive diffuse large B-cell lymphoma is a post-germinal center-type lymphoma without alterations in the CCND1 gene locus. *Leuk Lymphoma.* 2011;52(3):458-466.
- Martin-García D, Navarro A, Valdes-Mas R, et al. CCND2 and CCND3 hijack immunoglobulin light-chain enhancers in cyclin D1(-) mantle cell lymphoma. *Blood.* 2019;133(9):940-951.
- Bea S, Valdes-Mas R, Navarro A, et al. Landscape of somatic mutations and clonal evolution in mantle cell lymphoma. *Proc Natl Acad Sci U S A.* 2013;110(45):18250-18255.
- Nadeu F, Delgado J, Royo C, et al. Clinical impact of clonal and subclonal TP53, SF3B1, BIRC3, NOTCH1, and ATM mutations in chronic lymphocytic leukemia. *Blood.* 2016;127(17):2122-2130.
- King RL, McPhail ED, Meyer RG et al. False-negative rates for MYC fluorescence in situ hybridization probes in B-cell neoplasms. *Haematologica.* 2019;104(6):e248-e251.
- Yamamoto K, Okamura A, Inui Y, et al. Cryptic insertion of BCL2 gene into immunoglobulin heavy locus in follicular lymphoma with t(6;9)(p23;p13). *Leuk Res.* 2012;36(9):e202-205.
- Hilton LK, Tang J, Ben-Neriah S, et al. The double hit signature identifies double-hit diffuse large B-cell lymphoma with genetic events cryptic to FISH. *Blood.* 2019;134(18):1528-1532.
- Peterson JF, Baughn LB, Ketterling RP, et al. Characterization of a cryptic IGH/CCND1 rearrangement in a case of mantle cell lymphoma with negative CCND1 FISH studies. *Blood Adv.* 2019; 3(8):1298-1302.
- Ribera-Cortada I, Martinez D, Amador V, et al. Plasma cell and terminal B-cell differentiation in mantle cell lymphoma mainly occur in the SOX11-negative subtype. *Mod Pathol.* 2015;28(11):1435-1447.